Chemistry Africa (2023) 6:1699–1708
https://doi.org/10.1007/s42250-023-00606-6

REVIEW

Stress-Corrosion and Corrosion-Fatigue Properties of Surface-Treated Aluminium Alloys for Structural Applications

Temitope Olumide Olugbade[1] · Babatunde Olamide Omiyale[1] · Oluwole Timothy Ojo[1] · Michael Kanisuru Adeyeri[1]

Received: 13 November 2022 / Accepted: 22 January 2023 / Published online: 27 January 2023

Abstract

Aluminium alloys are materials of choice for structural applications with remarkable mechanical and corrosion properties but prone to premature failure under the combined action of stress and corrosive environment. Over the years, several efforts including surface modifications and thermomechanical treatments have been made to address this shortcoming. The present work reviews the corrosion, stress corrosion cracking (SCC), and corrosion fatigue (CF) behaviour of nanostructured Al alloys especially the Al–Mg (5xxx-series) and Al–Zn–Mg (7xxx-series), after surface modifications. To a large extent, the SCC behaviour of Al alloys could be influenced by the microstructure, heat treatments, stress, pre-strain, alloy compositions, and environments. The CF properties of surface-modified Al alloys were reviewed with a view to finding a relation between the nanostructured Al alloys and their aftermath corrosion fatigue properties. The fatigue behaviour of Al alloys can be influenced by the corrosion behaviour via various mechanisms including hydrogen embrittlement, prompt crack growth in aggressive environment, and crack initiation at pits. The strengthening mechanisms in nanostructured Al alloys are also briefly explained. For further study, some insights are then provided to avail the readers on options for future research.

Keywords Corrosion fatigue · Fatigue · Stress corrosion cracking (SCC) · Cracks · Stress

Abbreviations

CERTs	Constant-extension-rate tests
CRS	Compressive residual stress
DoS	Degree of sensitization
DPD	Dynamic plastic deformation
DSC	Differential scanning calorimetry
EIC	Environment-induced cracking
FSP	Friction stir processing
FSW	Friction stir welding
GBs	Grain boundaries
GBPs	Grain boundary precipitates
HAGBs	High angle grain boundaries
HCF	High-cycle fatigue
IGPs	Intragranular precipitates
IGSCC	Intergranular stress corrosion cracking
LAGBs	Low angle grain boundaries
NAMLT	Nitric acid mass loss test
UTS	Ultimate tensile strength
VHCF	Very-high-cycle fatigue
SCC	Stress corrosion cracking
SFE	Stacking fault energy
SLM	Selective laser melting
SMAT	Surface mechanical attrition treatment
SPD	Severe plastic deformation
SQA	Step-quench and aging
SSRT	Slow strain rate testing

✉ Temitope Olumide Olugbade
tkolugbade@futa.edu.ng

[1] Department of Industrial and Production Engineering, Federal University of Technology, P.M.B. 704, Akure, Ondo State, Nigeria

1 Introduction

Aluminum alloys, especially the Al–Mg (5xxx-series) and Al–Zn–Mg (7xxx-series) are presently receiving wide attention and interests as potential structural materials which find applications in most aerospace and automotive industries [1–3]. The uncommon interests cannot only be attributed to their high toughness and specific strength, but their low density and outstanding corrosion resistance performance [1, 2]. However, they are susceptible to stress corrosion cracking (SCC) especially in aggressive environments and this still remain a bottleneck limiting their applications in some areas. Efforts have been made to address the current SCC

challenge, and research is still ongoing to explore several feasible options.

Stress corrosion cracking (SCC) in Al alloys (an advanced generation of cracks leading to vital failure) often takes place when susceptible Al materials are subjected to the combined action of stress (above the limit) and corrosive environment. In short, a tensile stress condition beyond the limit, a specific environment and a susceptible Al metal are the three main factors influencing the occurrence of SCC in Al alloys i.e., SCC cannot probably occur if the three factors are not simultaneously present [2, 3]. The combination of these three factors often results in total failure and hence it should be avoided by all means for Al alloys. Moreover, SCC of Al alloys in corrosive environments occurs in three stages [4–6]: (a) crack initiation, originating from a smooth surface and depends to a large extent on the environment properties such as temperature, pH and salinity; metal structure and crack nucleation mechanism, (b) crack propagation, from the point of crack initiation to the core part of the materials under the combined action of applied tensile stress and corrosion mechanism, and (c) failure, which occurs when the limit has been exceeded by the combined corrosion—applied stress forces. It should be noted that both Al–Mg (5xxx-series) and Al–Zn–Mg (7xxx-series) are susceptible to SCC, and this often causes a catastrophic failure anytime it occurs in Al alloys especially the Al–Zn–Mg (7xxx-series). However, the imminent failure can be avoided or reduced to the lowest level by enhancing the SCC resistance via surface modifications [4, 7–14] and thermomechanical treatments. More details about these methods are given in section two.

The corrosion fatigue behaviors of Al alloys differ from each other in different environments and processing parameters after surface modifications [15–30]. Firstly, using the Pearson correlation analysis [15] and Trantina-Jonson model [16] by correlating parameters between the corrosion pits and equivalent cracks, the pre-corrosion fatigue lifetime [15] and corrosion fatigue crack growth rate [16] as well as the pit growth [17] in Al alloys can easily be predicted. Unravelling the effects of pre-corrosion on the fatigue lifetime of Al 8011 alloy [18], a significant decrease in the fatigue strength was observed due to the occurrence of corrosion pits on the sample surface. In addition, due to exfoliation, pit clustering, and pitting leading to localized corrosion damage characterized with crack initiation at corrosion defects, a similar decrease in fatigue lifetime was reported for AA6061 Al alloy [19] after surface treatment by friction stir welding (FSW) process. However, decreasing the pH value and increasing the corrosion solution flow rate, temperature, and corrosion time could reduce the fatigue lifetime of Al alloys, as illustrated for 2024-T4 Al alloy by Chen et al. [20].

In both 3.5% NaCl solution and air, there is an improvement in the corrosion fatigue properties of 7A85 Al alloy [21] after shot peening and plasma electrolytic oxidation, which can be linked to the compressive residual stress (CRS) induced by the shot peening treatment. Meanwhile, a large size of pits can occur by increasing the pre-corrosion time, resulting in reduced multiaxial fatigue lifetime, just as the case of 2024-T4 Al alloy [22, 23] in different corrosive environments. As indicated by Leon and Aghion [24] for Al alloy processed via selective laser melting (SLM), the corrosion fatigue resistance could be greatly improved in different corrosive environments by reducing the surface roughness. By this, surface defects like cavities and holes can be greatly reduced. All efforts must be made to reduce the surface and corrosion defects/pits [25] since they negatively affect the corrosion fatigue performance by causing premature crack initiation [26] and accelerating the rate of crack growth [27]. Investigating the effects of surface modifications by ball-burnishing and shot peening on the corrosion fatigue properties of AA5083 [28] in chloride environment, a significant improvement in the fatigue lifetime is obtained. Shot peening and ball-burnishing process also enhances the corrosion fatigue resistance of AA7075-T73 alloy [29]. The improvement in the corrosion fatigue performance can be accrued to the residual stress induced by the surface modification process, heat treatment and hardness increase through the addition of nano-clay particles [30], reducing the surface defects as well as the corrosion defects and pits in the process.

The present work reviews the corrosion, SCC, and CF properties of surface-modified Al alloys with a view to finding a relation between the nanostructured Al alloys and their aftermath corrosion fatigue properties, and most importantly proffer possible solutions to addressing the common catastrophic failure experienced by Al alloys under the combined actions of stress and corrosive environments.

2 SCC of Surface-Modified Al Alloys

For structural applications, Al alloys are very sought-after materials due to their versatility, strength, and corrosion properties. However, their applications and usability are often limited due to their susceptibility to SCC in aggressive environments. Several surface modifications including equal-channel angular pressing (ECAP), dynamic plastic deformation (DPD), shot peening or surface mechanical attrition treatment (SMAT) techniques have been successfully applied in the past to enhance the SCC resistance of different Al alloys in different environmental conditions [4, 7–14]. For instance, the SCC resistance of nanostructured AA 7075-T6 Al alloy via shot peening process [4] was significantly increased, although the surface roughness also increased in the process which promotes localized corrosion pitting. Here, the CRS induced by shot peening and refined microstructure inhibits the formation of pits and propagation of crack thereby enhancing the resistance to SCC, but at

the expense of the corrosion behaviour because the microstructural change often acts as a pitting corrosion site during the process. The negative effects of the surface roughness may be checked and addressed by adjusting the shot peening intensity and shot diameter during the process.

Similarly, the fatigue resistance of 7075 Al alloy [7] was reportedly enhanced after ultrasonic rolling which can again be accrued to the large values of CRS induced during the process on the surface layer of the Al alloy. It can be said here that the higher the induced CRS, the higher the resistance to fatigue and SCC. At the same time, the maximum CRS and CRS thickness layer increases with increasing roller radius, amplitude, and static load. In addition, Pan et al. [8] reported a significant increment in the localized corrosion resistance for surface modified AA7075 alloys due to the precipitation mechanism, unique surface properties and microstructures [1] which gives room for improvement of surface properties, however, the effects of nanoparticles during the treatment on the fatigue and SCC of AA7075 Al alloys could not be ascertained.

As reported by Xu et al. [9], after sensitization, the nanostructured Al–5Mg via DPD process experienced a significant increase in resistance to SCC and intergranular corrosion (IC) as well as an improved ductility and strength, when compared with its coarse-grained counterpart. This is in relation with the generation of a high volume of low-angle grain boundaries (LAGBs) through the DPD process. Meanwhile, estimating the SCC susceptibility of nanostructured AA5083 via friction stir processing (FSP) in 0.6 M NaCl solution [10] using slow strain rate testing (SSRT) method [10, 11], the FSP-processed AA5083 revealed no susceptibility while the ultrafine grained Al–Mg–Sc–Zr showed high SCC susceptibility. A similar case was reported for Al–Zn–Mg–Cu alloy (AA7075) [12–14] especially after surface treatment by high pressure torsion method [14].

Just like shot peening process, SMAT technique has also be widely adopted to influence the general corrosion properties of materials without tampering with their inherent properties [31–38]. More importantly, the positive influence of SMAT on the SCC resistance of Al alloys has been reported [39–43]. After surface modification via SMAT technique, Li et al. [39] reported a significant increase in SCC resistance of alloy 690 in alkaline steam generator environments. This may be related to the remarkable CRS induced by SMAT technique and the aftermath formation of stable film. In addition, the ultra-fine microstructures play a vital role in the improvement of pitting corrosion resistance observed for nanostructured Al–8.6Mg and Al–7.5Mg Al alloys [40] in artificial and natural environments, as well as other Al alloys [41–43]. In short, the SCC behaviour of nanostructured Al alloys could be influenced by the environments, alloy compositions, pre-strain, stress, heat treatments, and microstructure.

3 Corrosion Fatigue Properties of Nanostructured Al Alloys

Among the mechanical properties of materials, the fatigue property has always been one of the most important issues defining the ability of materials to resist failure in very-high-cycle fatigue (VHCF) and high-cycle fatigue (HCF) conditions [44–50]. Obviously, the mechanical properties of Al alloys are enhanced after surface modifications in terms of yield strength ($\sigma_{0.2}$ (MPa)), ultimate tensile strength (UTS) (σ_b (MPa)), and percentage elongation (δ (%)) [26, 51–65], as summarized in Table 1. The formation of nanostructured layer via grain refinement mostly prevents the fatigue crack initiation and propagation. This is made possible by the presence of the larger volume fraction of grain boundaries impeding the dislocation sliding and hence preventing the initiation of cracks, and the nanostructured layer is believed to be the primary factor hindering the creation of stress concentrator for initiation of crack [66–73]. The surface quality goes a long way in determining the strength of the materials after surface treatment. In addition, plastic deformation could induce microcracks on the sample surface reducing the fatigue strength of materials resulting in the stress concentration and initiation of cracks [74–79]. In short, microcracks induced by severe plastic deformation (SPD) can lead to micro damage on sample surface leading to multi-crack initiation phenomenon [54]. However, it is important to note that once the crack breaks through the SPD layer and reaches a baser metal structure, then the SPD layer will have no significance influence again—this is a known issue with laser surface modified layers. Furthermore, the fatigue strength of severely plastic deformed materials is expected to improve via the CRS by hindering crack initiation and propagation [80–85], i.e., CRS can enhance the resistance of crack initiation and propagation.

Interestingly, the SMAT technique has been in the frontline among other SPD methods in significantly enhancing the fatigue strength as well as the corrosion resistance of materials [90–96]. Several factors such as phase transformation, nanocrystalline layer, surface layer, and residual stress and its relaxation [54] could contribute to the effects of SMAT on the fatigue strength of Al alloys. The deformation-induced phase transformation has significant influence on the properties of materials of Al alloys and steels in particular. Under the effect of plastic deformation, a transition of a fraction of austenitic phase to martensitic phase can occur. By this, the fatigue strength of materials can be enhanced by the martensitic transformation induced by SMAT together with the formation of gradient-structured layers since the martensitic phase tends to have higher mechanical strength than the austenitic phase.

Table 1 Mechanical properties of nanostructured Al alloy after exposure in different corrosive environments

Materials	Corrosive environments	Routes	$\sigma_{0.2}$ (MPa)	σ_b (MPa)	δ (%)	Refs.
Al–7.5Mg	3.5 wt% NaCl solution, 25 °C	Cryomilling + hot isostatic pressing	545	580		[51]
Al–8.6Mg	3.5 wt% NaCl solution, 25 °C	Cryomilling + hot isostatic pressing	525	600		[51]
7A85 Al Alloy	20 g L^{-1} CrO_3 and 50 mL L^{-1} H_3PO_4, 80 °C		370.3	413.3	1.86	[52]
Al–Zn–Mg–Cu	1.0 M NaCl + 0.01 M H_2O_2; for 6 h; at 30 ± 1 °C			645	11.20	[55]
Al–Mg–Si	0.5 M NaCl, 25 °C	ECAP	243	253	11.40	[56]
Al–Mg–Si	0.5 M NaCl, 25 °C	ECAP	222	238	13.20	[56]
Al–7.5Mg		Cryomilling	553	665	4.20	[57]
Al5083	Air	ECAP	96	261	15.41	[58]
Al5083	3.5% NaCl	ECAP	155	246	10.77	[58]
7B50-T7751	3.5 wt% NaCl	USRP	531.5	574.1	10.95	[59]
7B50-T7751	3.5 wt% NaCl	USRP	512.4	577.7	0.10	[60]
7075-T651	3.5 wt% NaCl		469	538	7.00	[26]
Al–5%Mg	Air	DPD	263	353	31.00	[9]
Al–5%Mg	NaCl	DPD	260	350	29.70	[9]
AA7075		HPT	978	1010	5.00	[62]
AA7075		ECAP	399	442	2.40	[63]
AA7075		Cryorolling	599	602	5.00	[64]
7075-T6	Natural seawater		505	573	11.00	[86]
5456-H116	Natural seawater		398	534	14.00	[86]
1050	Natural seawater		104	108	10.00	[86]
Al–0.2Fe–0.07La	3.5% NaCl		196	213	1.30	[87]
Al–0.1Fe–0.07La	3.5% NaCl		170	180	1.07	[87]
Al–0.07Fe–0.07La	3.5% NaCl		129	134	0.69	[87]
Al–1Zn	3 g NaCl + 1 mL HCl + 97 mL H_2O	ECAP	35	110	55.00	[88]
Al–2Zn	3 g NaCl + 1 mL HCl + 97 mL H_2O	ECAP	40	115	60.00	[88]
Al–3Zn	3 g NaCl + 1 mL HCl + 97 mL H_2O	ECAP	60	120	50.00	[88]
7055	3.5 wt% NaCl		580	643	9.20	[89]
7055-Pr	3.5 wt% NaCl		573	628	14.30	[89]
7055-Er	3.5 wt% NaCl		596	665	12.50	[89]
7055-Pr–Er	3.5 wt% NaCl		590	654	12.90	[89]

Studies on the fatigue crack growth and tensile properties of the nanostructured and ultrafine-grained Al alloys have been carried out in the past [54–57, 97–106]. As a function of environment, the corrosion fatigue properties of nanostructured Al alloys can be grouped into crack initiation, low-rate growth, high-rate growth, and rupture. And it can be studied in line with corrosion product, crack propagation, pit location and initiation. The corrosion fatigue strengths of Al alloys can be significantly enhanced with the adoption of SPD techniques such as SMAT [41, 42, 54] and shot peening [4, 21]. The fatigue behaviour of Al alloys can be influenced by the corrosion behaviour via various mechanisms including hydrogen embrittlement/SCC [57, 97–101], prompt crack growth in aggressive environment [102], and crack initiation at pits [102–106]. In the case of nanostructured 2024 Al alloy processed via SMAT technique, the enhancement in the corrosion resistance property is related to the formation of a dense passive film as a result of nano structuring effect of SMAT and protective coating from microarc oxidation process (post-SMAT) [107]. The fabrication of the nanostructured layer at the bottom of the coating is expected to significantly enhance the general corrosion resistance property.

As summarized in Table 2, the corrosion fatigue mechanisms of nanostructured Al alloys in different corrosive environments and applications can be categorized in terms of induced CRS, cleavage and fracture, nucleation of pores, precipitate-free zone width, pitting kinetics, quench rate, distribution of precipitates, grain boundary precipitates, matrix precipitate, and enhanced passivation [1, 52, 55, 56, 108–111]. Under corrosion fatigue conditions, attributed to the premature crack initiation on corrosion defects, the conventionally processed alloys exhibit a reduced fatigue lifetime. The reduced fatigue strength can be explained based on different mechanisms including

Table 2 Corrosion fatigue properties of nanostructured Al alloys in different corrosive environments and applications

Materials	Environments	Processing methods	Fatigue limit (MPa)	Loading cycles	Corrosion methods	Application/ environment	Corrosion mechanism	Refs.
Al–7.5Mg	Air Seawater	Cryomilling + hot isostatic pressing	276	10^7	Corrosion fatigue	Marine and naval	Enhanced passivation	[108]
Al–7.5Mg	3.5% NaCl solution	Cryomilling + hot isostatic pressing			SCC	Naval	Pitting kinetics	[51]
7A85-T7452 Al Alloy	Air 3.5 wt% NaCl, 25 °C		400	5×10^6	Corrosion fatigue	Marine	Matrix and anodic grain boundary precipitates	[109]
7A85 Al Alloy	20 g L^{-1} CrO_3 + 50 mL L^{-1} H_3PO_4, 10 min, 80 °C				Weight loss	Industrial-marine	Grain boundary precipitates	[52]
Al–Zn–Mg–Cu	1.0 M NaCl + 0.01 M H_2O_2; for 6 h; at 30 ± 1 °C				Stress corrosion cracking		Distribution of precipitates Quench rate Precipitate-free zone width	[55]
Al–8.6Mg	3.5% NaCl	Cryomilling + hot isostatic pressing					Pitting kinetics	[51]
Al–Mg–Si	0.5 M NaCl, 25 °C	ECAP		10^6	Corrosion fatigue			[56]
7075-T651 Al	0.1 M NaCl, $R = 0.05$	Shot peening	370	10^7	Corrosion fatigue		Induced compressive residual stresses	[110]
2524-T3 Al Alloy	$R = 0$, 3.5% NaCl		495 (horizontal) 523 (longitudinal)	10^6	Corrosion fatigue	Automotive	Cleavage and fracture, nucleation of pores	[1]

hydrogen embrittlement at defect and plastic deformation localization around the corrosion defects [56].

As revealed in Fig. 1a–f, the corrosion fatigue performance of Al alloys is influenced by the gradient-structured layers produced on the top layers, in different environment and conditions. For instance, the nanostructured 7B50-T7751 Al alloy processed by USRP (Fig. 1a, b, e) [59, 60] exhibits an improved corrosion fatigue life with optimal surface integrity in air and 3.5% NaCl as compared with the conventional Al alloy [59]. This is achievable due to the microstructure refinement and CRS induced by USRP, inhibiting the appearance and formation of intergranular and pitting corrosion thereby preventing the initiation of corrosion fatigue cracks. As a matter of fact, gradient structure is a contributing factor for the improvement in corrosion fatigue performance [60]. Hence, the study on the influence of surface integrity as well as the combined effect of surface nanocrystallization and CRS is important as far as the corrosion fatigue life of Al alloy is concerned. As indicated in Fig. 1c [1], the fatigue fracture morphology can occur in corrosion pitting, fatigue crack propagation, and rapid fatigue fracture regions. In addition, the fatigue life increases mostly with surface nanocrystallization [59], and corrosion fatigue can set in for conventional Al alloys without gradient structures (Fig. 1f) [108]. Generally, reduction in fatigue strength of Al alloys, for instance 7075-T651 [26] and AlLi alloy 2090 [98], can mainly be attributed to the combined effects of hydrogen embrittlement and anodic dissolution at the crack tip, as well as the formation of corrosion pits [26]. Hence, hydrogen embrittlement remains one of the primary mechanisms for the corrosion fatigue process of Al alloys.

There is a direct relationship between the corrosion and mechanical properties of Al alloys as illustrated in Fig. 2. In the process of enhancing the corrosion resistance

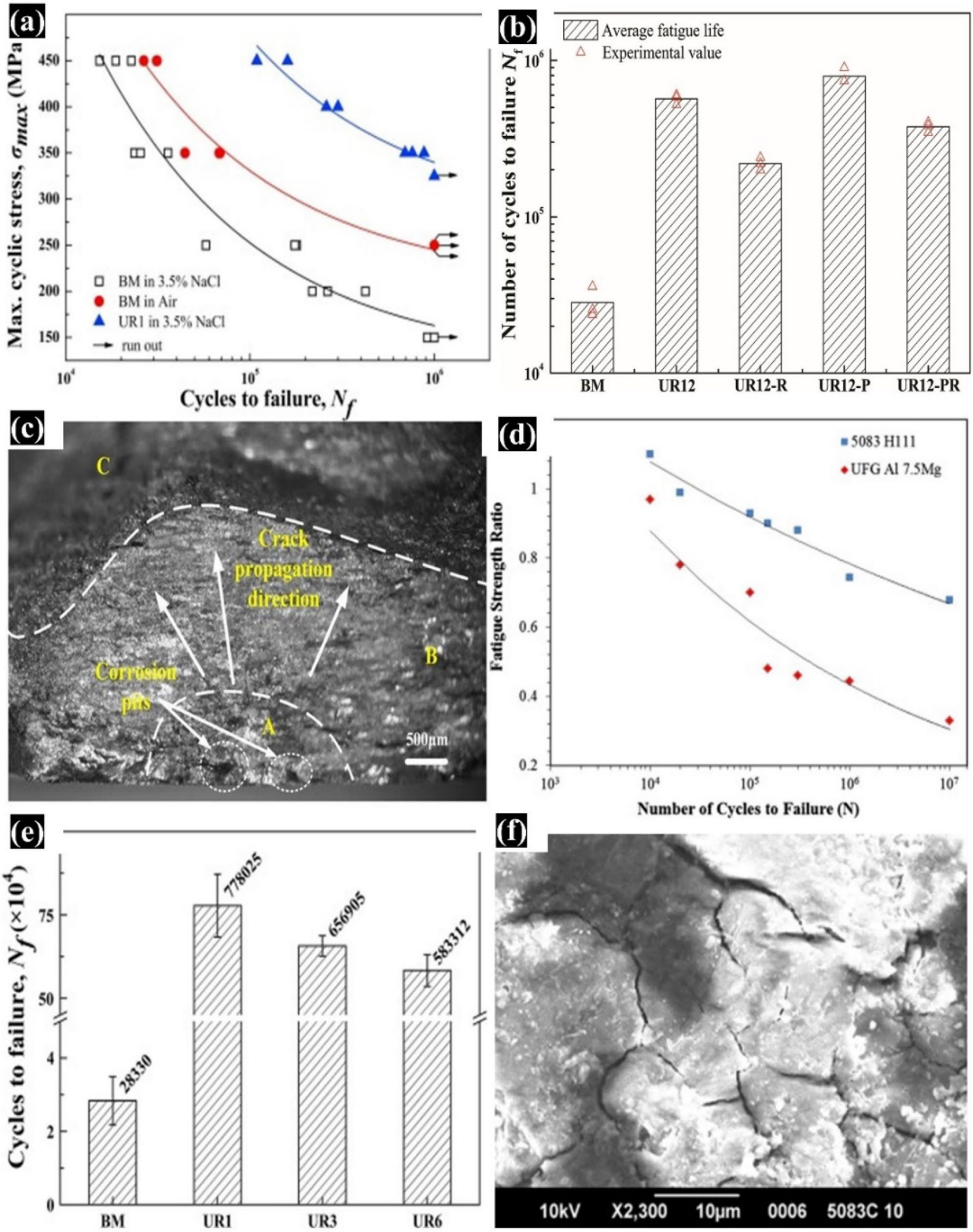
(a)
Max. cyclic stress, σ_{max} (MPa
Cycles to failure, N_f
BM in 3.5% NaCl
BM in Air
UR1 in 3.5% NaCl
run out
(b)
Average fatigue life
Experimental value
Number of cycles to failure N_f
BM
UR12
UR12-R
UR12-P
UR12-PR
(c)
C
Crack propagation direction
Corrosion pits
A
B
500μm
(d)
5083 H111
UFG Al 7.5Mg
Fatigue Strength Ratio
Number of Cycles to Failure (N)
(e)
Cycles to failure, N_f(×10^4)
28330
778025
656905
583312
BM
UR1
UR3
UR6
(f)
10kV X2,300 10μm 0006 5083C 10

◂**Fig. 1** Corrosion fatigue performance of gradient-structured Al alloys in different environment and conditions; **a** S–N curves of 7B50-T7751 Al alloy processed by USRP in air and 3.5% NaCl [59], **b** corrosion fatigue life of 7B50-T7751 processed via USRP in 3.5% NaCl [60], **c** corrosion morphology of fractured 2524-T3 Al alloy in 3.5% NaCl [1], **d** fatigue strength of 5083 H111 and UFG Al–7.5Mg alloys processed via Cryomilling in 3.5% NaCl [108], **e** fatigue performance of 7B50-T7751 Al alloy processed by USRP in air and 3.5% NaCl [59], **f** corrosion fatigue of 5083 Al alloy processed via Cryomilling revealing anodic dissolution in 3.5% NaCl [108]

performance, it is necessary to ensure that the strength is not affected. However, the yield strength vs corrosion current density (i_{corr}) varies among the Al alloys. The 7055 Al alloy [89] experiences high yield strength together with the lowest i_{corr} (possibly signifying a good corrosion resistance property), but the case is different for 1050 Al alloy [86] with low yield strength even though a good corrosion resistance property is obtained. A similar improvement in both the strength and corrosion resistance can be observed for 7085 [67] and 7075-T6 [86] Al alloys. It can be seen that Al–0.07Fe–0.007La and Al–0.07Fe–0.007La Al alloys [87] possessed the highest i_{corr}, indicating a possible poor corrosion resistance performance and lowest yield strengths. The difference in behaviour of the yield strength vs corrosion resistance among the different types of Al alloys may be linked to the nature and extent of heat treatment, alloying compositions, or environmental factors [67, 71, 78, 81, 86–89].

On the other hand, thermomechanical treatments including the step-quench aging (SQA) and slow quench rate methods as well as electrodeposition/coatings and heat treatments, are widely receiving great attention as alternative methods of enhancing the overall properties of materials [112–119], especially the resistance of Al alloys to SCC [44–50]. To be specific, the SQA heat treatment reportedly increased the resistance of AA7097 Al alloy to SCC, which is probably due to the discontinuous distribution, large size, and high Cu content grain boundary precipitates [44]. In addition, the thermomechanical treatment via slow quench rate decreases the rate of crack propagation thereby improving the resistance of AlZnMgCu alloy [45] to SCC.

4 Strengthening Mechanisms in Nanostructured Al Alloys

The susceptibility to corrosion of Al alloy differs among the various classes. For example, Al–Mg (5xxx-series) and Al–Zn–Mg (7xxx-series) have very different behaviors under the same electrolyte and applied electrochemical potential conditions due to differences in the underlying mechanisms responsible for susceptibility.

4.1 Al–Mg (5xxx-Series)

Due to their excellent corrosion resistance and mechanical properties, good weldability, high strength/weight ratio, and low cost, non-heat treatable Al–Mg 5xxx alloys have been widely accepted as the preferred materials of choice for structural applications especially in aggressive marine conditions. They also find applications in forging, transport, and shipbuilding industries, as well in aerospace and building sectors. Aluminium (Al) and magnesium (Mg) are the two main alloying elements in these alloys, and the presence of Mg plays a vital role in achieving the stated properties by enhancing the mechanical properties and stimulating solid solution and work hardening strengthening. However, the Mg element in the alloy does not alter the deformation features and tamper with the SFE of Al–Mg 5xxx, but can result in lattice distortion, hasting the strain hardening in the process. Under standard service temperatures (60–200 °C), over a long period of time, these alloys often experience sensitization and more susceptibility to intergranular stress corrosion cracking (IGSCC) when the Mg content in them is above 3 wt%, compared to the standard alloy composition. The sensitivity to IGSCC can be established by constant-extension-rate tests (CERTs) and be assessed based on the mass losses via nitric acid mass loss test (NAMLT). Furthermore, findings revealed that the IGSCC in Al–Mg–5xxx is arguably related to the occurrence of the Mg-rich β phase—Al_3Mg_2 precipitates [120–123] along the grain boundaries at elevated temperatures, and it could be greatly influenced by the time and orientation of exposure/grain boundary, grain size as well as the degree of sensitization (DoS) [123–125].

The strengthening mechanisms of nanostructured Al Alloys majorly comprise the grain boundary, solution hardening, precipitation strengthening, and dislocation strengthening. As a matter of fact, the strain hardening, and solid solution strengthening are the major source of strength in Al–Mg–5xxx alloys [126, 127].

4.2 Al–Zn–Mg (7xxx-Series)

Al-Zn-Mg (7xxx-series) are known for their high strength, moderate heat and electrical conductivities, high strength/density ratio, good workability, and enhanced corrosion properties, which makes them promising materials for aluminium sheets for different applications as well as extrusions for aircrafts and automotive parts [128–130]. This remarkable feat can be linked to the presence of considerable and desired alloying elements—Mg and Zn, which improves the mechanical properties and stimulates the precipitation hardening mechanism [128, 131]. However, their maximum strengths can be obtained at low temperatures because at high temperatures, they are prone to stress corrosion and over-ageing. The Al–Zn–Mg 7xxx are heat treatable alloys

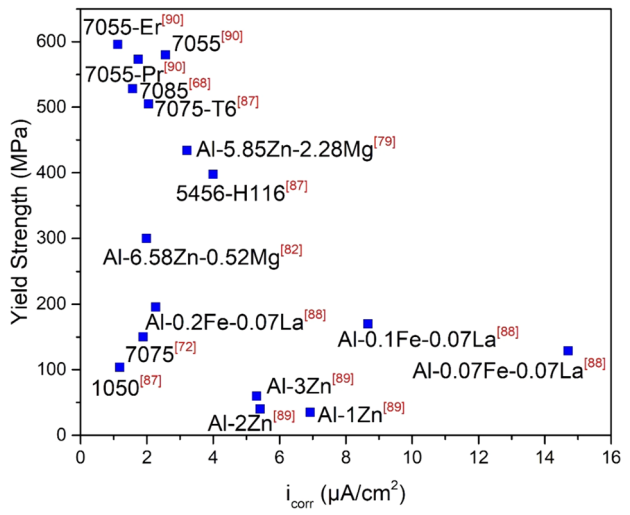

Fig. 2 Relationship between the yield strength and corrosion current density (i_{corr}) of fine-grained Al alloys, data compiled from [67, 71, 78, 81, 86–89]

which can be strengthened by precipitation or age hardening, unlike the Al–Mg–5xxx series which can be reinforced by cold working process and are non-heat treatable.

5 Summary and Future Work

The corrosion, stress corrosion cracking (SCC) resistance, and corrosion fatigue (CF) behaviour of nanostructured Al alloys especially the Al–Mg (5xxx-series) and Al–Zn–Mg (7xxx-series) have been reviewed. These alloys are widely useful for aerospace and automotive applications [131–139] because of their high specific strength and excellent corrosion resistance but very prone to SCC especially in harsh service conditions. The imminent catastrophic failure can be avoided or reduced by enhancing the SCC resistance via surface modifications and thermomechanical treatments such as step-quench aging (SQA) and slow quench rate.

Al and Mg are the two main alloying elements in Al–Mg (5xxx-series). The presence of Mg does not alter the deformation features or tamper with the stacking fault energy (SFE) hence play a vital role in achieving the remarkable surface properties, but can result in lattice distortion, hasting the strain hardening in the process. Additionally, the improved SCC and CF resistance experienced by the Al-Zn-Mg (7xxx-series) can be linked to the presence of considerable and desired alloying elements—Mg and Zn, which improves the mechanical properties and stimulates the precipitation hardening mechanism, but they are prone to stress corrosion and over-ageing at high temperatures. Moreover, the Al–Mg–5xxx series can be reinforced by cold working process and are non-heat treatable, compared to the Al–Zn–Mg 7xxx which are heat treatable alloys and can be strengthened by precipitation or age hardening.

An improvement in the SCC and CR resistance of Al alloys is achievable due to the microstructure refinement and compressive residual stress (CRS) induced during the surface modification process, inhibiting the appearance and formation of intergranular and pitting corrosion thereby preventing the initiation of corrosion fatigue cracks. By this, gradient structure plays an important role in enhancing the corrosion fatigue performance. In addition, the rate of crack propagation can be decreased thereby increasing the resistance of Al alloys to SCC via the thermomechanical treatments, and this is probably attributed to the discontinuous distribution, large size, and high Cu content grain boundary precipitates. Hence, the SCC behaviour of nanostructured Al alloys could be influenced by the environments, alloy compositions, pre-strain, stress, heat treatments, and microstructure. Furthermore, the corrosion fatigue mechanisms of nanostructured Al alloys in different corrosive environments can be categorized in terms of induced CRS, cleavage and fracture, nucleation of pores, precipitate-free zone width, pitting kinetics, quench rate, distribution of precipitates, and enhanced passivation.

The corrosion, stress corrosion cracking (SCC), and corrosion fatigue (CF) behavior differs among the various classes of Al alloy. For example, Al–Mg (5xxx-series) and Al–Zn–Mg (7xxx-series) have very different behaviors under the same electrolyte and applied electrochemical potential conditions due to differences in the underlying mechanisms responsible for susceptibility. For future study, further works on the underlying mechanisms responsible for susceptibility in various classes of Al alloys in relation to their corrosion, SCC, and CF behaviors after surface modification can be carried out, and most importantly the influence of surface modification on the causal factors responsible for susceptibility.

Declarations

Conflict of Interest The authors report no conflict of interest.

References

1. Liu C, Ma L, Zhang Z, Fu Z, Liu L (2021) Metals 11:1754
2. Abolhasani A, Langelier B, Worswick MJ, Wells MA, Esmaeili S (2022) J Alloy Compd 906:164344
3. Kayani SH, Park S, Euh K, BokSeol J, GiKim J, Sung H (2022) Mater Charact 190:112019
4. Bao L, Li K, Zheng J, Zhang Y, Zhan K, Yang Z, Zhao B, Ji V (2022) Surf Coat Technol 440:128481
5. Umamaheshwerrao AC, Vasu V, Govindaraju M, Saisrinadh KV (2016) Trans Nonferrous Met Soc China 26:1447–1471
6. Pedeferri P (2018) Springer, Cham. https://doi.org/10.1007/978-3-319-97625-9_13

7. Zheng J, Shang Y, Guo Y, Deng H, Jia L (2022) J Manuf Process 80:132–140
8. Pan S, Yuan J, Linsley C, Liu J, Li X (2022) Corros Sci 206:110479
9. Xu W, Xin YC, Zhang B, Li XY (2022) Acta Mater 225:117607
10. Argade G, Kumar N, Mishra R (2013) Mater Sci Eng A 565:80–89
11. Holroyd NH, Burnett T, Seifi M, Lewandowski JJ (2017) Mater Sci Eng A 682:613–621
12. Knight SP, Birbilis N, Muddle BC, Trueman AR, Lynch SP (2010) Corros Sci 52:4073–4080
13. Knight SP, Pohl K, Holroyd NJH, Birbilis N, Rometsch PA, Muddle BC, Goswami R, Lynch SP (2015) Corros Sci 98:50–62
14. Zhang Y, Jin S, Trimby PW, Liao X, Murashkin MY, Valiev RZ, Liu J, Cairney JM, Ringer SP, Sha G (2019) Acta Mater 162:19–32
15. Huang Y, Ye X, Hu B, Chen L (2016) Int J Fatigue 88:217–226
16. Wang CQ, Xiong JJ, Shenoi RA, Liu MD, Liu JZ (2016) Int J Fatigue 83:280–287
17. Hu P, Meng Q, Hu W, Shen F, Zhan Z, Sun L (2016) Corros Sci 113:78–90
18. Mishra RK (2020) Mater Today Proc 25(4):602–609
19. Rodriguez RI, Jordon JB, Allison PG, Rushing T, Garcia L (2019) Mater Sci Eng A 742:255–268
20. Chen Y, Liu Ch, Zhou J, Wang F (2019) J Alloy Compd 772:1–14
21. Yea Z, Liu D, Zhang X, Wu Z, Long F (2019) Appl Surf Sci 486:72–79
22. Chen Y, Liu CH, Zhou J, Wang X (2017) Int J Fatigue 98:269–278
23. Chen Y, Zhou J, Liu Ch, Wang F (2018) Int J Fatigue 108:35–46
24. Leon A, Aghio E (2017) Mater Charact 131:188–194
25. Guerin M, Alexis J, Andrieu E, Blanc C, Odemer G (2015) Mater Des 87:681–669
26. Chlistovsky RM, Heffernan PJ, DuQuesnay DL (2007) Int J Fatigue 29:1941–1949
27. Meng X, Lin Z, Wang F (2013) Mater Des 51:683–687
28. Abdulstaar M, Mhaede M, Wollmann M, Wagner L (2014) Surf Coat Technol 254:244
29. Mhaede M (2012) Mater Des 41:61–66
30. Aroo H, Azadi M, Azadi M (2022) Silicon 14:3749–3763
31. Olugbade T, Lu J (2018) In: Twelfth international conference on fatigue damage of structural materials, Cape Cod, Hyannis, USA
32. Olugbade TO, Lu J (2020) Nano Mater Sci 2:3–31
33. Olugbade T (2019) Data-in-Brief 25:104033
34. Olugbade T, Liu C, Lu J (2019) Adv Eng Mater 21:1900125
35. Olugbade TO, Lu J (2019) Anal Lett 52:2454–2471
36. Olugbade TO, Olutomilola EO, Olorunfemi BJ (2022) Corros Rev 40:189–203
37. Olugbade TO, Omiyale BO, Ojo OT (2022) J Mater Eng Perform 31:1707–1727
38. Olugbade TO, Lu J (2019) J Bio Tribo Corros 5:38
39. Li N, Shi S, Luo J, Lu J, Wang N (2016) Mater Res Lett 4:180–184
40. Sharma MM, Ziemian CW (2008) J Mater Eng Perform 17:870–878
41. DeOrio J (2020) Barrett. The Honors College Thesis/Creative Project Collection
42. Wen L, Wang Y, Zhou Y, Guo LX, Ouyang JH (2011) Mater Chem Phys 126:301–309
43. Sharma MM, Tomedi JD, Weigley TJ (2014) Mater Sci Eng A 619:35–46
44. Xie P, Chen S, Chen K, Jiao H, Huang L, Zhang Z, Yang Z (2019) Corros Sci 161:108184
45. Yuan D, Chen K, Chen S, Zhou L, Chang J, Huang L, Yi Y (2019) Mater Des 164:107558
46. Olugbade TO, Abioye TE, Farayibi PK, Olaiya NG, Omiyale BO, Ogedengbe TI (2021) Anal Lett 54:1588–1602
47. Ou BL, Yang JG, Wei MY (2007) Metall Mater Trans A 38:1760–1773
48. Yang JG, Ou BL (2001) Scand J Metall 30:158–167
49. Olugbade TO, Omoniyi OO, Omiyale BO (2022) J Inst Eng (India) Ser D 103:141–147
50. Lin JC, Liao HL, Jehng WD, Chang CH, Lee SL (2006) Corros Sci 48:3139–3156
51. Strehblow HH (1995) Mechanisms of pitting corrosion. Corrosion mechanisms in theory and practice, Marcel Dekker, New York, pp 201–238
52. Olugbade T, Lu J (2020) In: International conference on nanostructured materials (NANO 2020), vol 117, Australia
53. Gupta RK, Fabijanic D, Dorin T, Qiu Y, Wang JT, Birbilis N (2015) Mater Des 84:270–276
54. Suresh S (1998) Fatigue of materials, 2nd edn. Cambridge University Press, Cambridge
55. Olugbade TO (2020) Corros Rev 38:473–488
56. Rochet C, Andrieu E, Arfaei B, Harouard JP, Laurino A, Lowe TC, Odemer G, Blanc C (2020) Int J Fatigue 140:105812
57. Pao PS, Jones HN, Cheng SF, Feng CR (2005) Int J Fatigue 27:1164–1169
58. Tellkamp VL, Lavernia EJ (1999) Nanostruct Mater 12:249–254
59. Xu X, Liu D, Zhang X, Liu C, Liu D, Zhang W (2019) Int J Fatigue 125:237–248
60. Xu X, Liu D, Zhang X, Liu C, Liu D (2020) J Mater Sci Technol 40:88–98
61. Ebrahimi M, Gode C, Attarilar S et al (2021) Trans Indian Inst Met 74:753–766
62. Liddicoat PV, Liao XZ, Zhao YH, Zhu YT, Murashkin MY, Lavernia EJ, Valiev RZ, Ringer SP (2010) Nat Commun 1:63
63. Cepeda-Jimenez CM, Garcia-Infanta JM, Ruano OA, Carreno F (2011) J Alloys Compd 509:8649–8656
64. Panigrahi SK, Jayaganthan R (2011) Mater Des 32:3150–3160
65. Ning AL, Liu ZY, Peng BS, Zeng SM (2007) Trans Nonferrous Met Soc China 17:1005–1011
66. Li J, Birbilis N, Li C, Jia Z, Cai B, Zheng Z (2009) Mater Char 60:1334–1341
67. Chen S, Chen K, Peng G, Jia L, Dong P (2012) Mater Des 35:93–98
68. Xu D, Birbilis N, Rometsch P (2012) Corrosion Sci 54:17–25
69. Ranganatha R, Kumar VA, Nandi VS, Bhat R, Muralidhara B (2013) Trans Nonferrous Met Soc China 23:1570–1575
70. Xie L, Lei Q, Wang M, Sheng X, Li Z (2017) J Mater Res 32:1105–1117
71. Jeshvaghani RA, Zohdi H, Shahverdi H, Bozorg M, Hadavi S (2012) Mater Char 73:8–15
72. Lei C, Li H, Fu J, Shi N, Zheng G, Bian T (2018) Metals 8:285
73. Wang Y, Jiang H, Li Z, Yan D, Zhang D, Rong L (2017) J Mater Sci Technol 34:1250–1257
74. Peng X, Li Y, Liang X, Guo Q, Xu G, Peng Y, Yin Z (2018) J Alloys Compd 735:964–974
75. Peng X, Guo Q, Liang X, Deng Y, Gu Y, Xu G, Yin Z (2017) Mater Sci Eng A 688:146–154
76. Liu Y, Liang S, Jiang D (2016) J Alloys Compd 689:632–640
77. Jiang J, Tang Q, Yang L, Zhang K, Yuan S, Zhen L (2016) J Mater Process Technol 227:110–116
78. Jiang D, Liu Y, Liang S, Xie W (2016) J Alloys Compd 681:57–65
79. Liu Y, Jiang D, Li B, Yang W, Hu J (2014) Mater Des 57:79–86
80. Wen K, Fan Y, Wang G, Jin L, Li X, Li Z, Zhang Y, Xiong B (2017) Prog Nat Sci Mater Int 27:217–227
81. Chen S, Li J, Hu GY, Chen K, Huang L (2018) J Alloys Compd 757:259–264

82. Zhang M, Liu T, He C, Ding J, Liu E, Shi C, Li J, Zhao N (2016) J Alloys Compd 658:946–951
83. Gao T, Zhang Y, Liu X (2014) Mater Sci Eng A 598:293–298
84. Wen K, Xiong B, Zhang Y, Li Z, Li X, Huang S, Yan L, Yan H, Liu H (2018) Met Mater Int 24:1–12
85. Li C, Pan Q, Shi Y, Wang Y, Li B (2014) Mater Des 55:551–559
86. Kim SJ, Ko JY (2006) Korean J Chem Eng 23:847–853
87. Yang X, Ding D, Xu Y, Zhang W, Gao Y, Wu Z, Chen G, Chen R, Huang, Tang J (2019) Metals 9: 706
88. Chuvil'deev VN, Nokhrin AV, Kopylov VI, Gryaznov MY, Shotin SV, Likhnitskii CV, Kozlova NA, Shadrina YS, Berendeev NN, Melekhin NV, Nagicheva GS, Smetanina KE, Tabachkova NY (2022) J Alloy Compd 891:162110
89. Zhong H, Li S, Zhang Z, Dehua Li, Deng H, Chen J, Qi L, Ojo OA (2022) Mater Today Commun 31:103732
90. Olugbade TO (2020) PhD thesis. Department of Mechanical Engineering, City University of Hong Kong
91. Olugbade TO (2022) MRS Adv 7:886
92. Olugbade TO, Omiyale BO (2021) Anal Techn Szegedinensia 15:9
93. Olugbade TO (2022) In: Singh M (ed) Stainless steel. IntechOpen Publisher, London
94. Olugbade TO (2021) Anal Lett 54:1055
95. Olugbade TO, Omiyale BO (2022) Chem Afr 5:1663
96. Olugbade TO (2022) Chem Afr 5:333
97. Ebtehaj K, Hardie D, Parkins RN (1989) Br Corros J 24:183–188
98. Dervenis CP, Meletis EI, Hochman RF (1988) Mater Sci Eng A 102:151–160
99. Pao PS, Jones HN, Gill SJ, Feng CR (2003) MRS Symp Proc 740:15–20
100. Haase I, Nocke K, Worch H, Zouhar G, Tempus G (2001) Prakt Metallogr 38:119–137
101. Elboujdaini M, Shehata MT (1997) Microstruct Sci 25:41–49
102. Wei RP, Harlow GD (1998) Corrosion and corrosion fatigue of aluminum alloys: chemistry, micromechanics, and reliability. Air Force Office of Scientific Research
103. Zamber JE, Hillberry BM (1999) AIAA J 37:1311–1317
104. Harlow DG, Wei RP (1998) Eng Fract Mech 59:305–325
105. Genel K (2007) Scr Mater 57:297–300
106. Tsai TC, Chuang TH (1997) Mater Sci Eng A 225:135–144
107. Wen L, Wang Y, Zhou Y, Guo L, Ouyang J (2011) Corros Sci 53:473–480
108. Sharma MM, Tomedi JD, Parks JM (2015) Corros Sci 93:180–190
109. Olugbade TO, Ojo OT, Omiyale BO, Olutomilola EO, Olorunfemi BJ (2021) J Braz Soc Mech Sci Eng 43:421
110. Zupanc U, Grum J (2010) J Mater Process Technol 210:1197–1202
111. Wei RP, Liao CM, Gao M (1998) Metall Mater Trans A 29A:1153–1160
112. Dang C, Yao Y, Olugbade TO, Li J, Wang L (2018) Thin Solid Films 653:107
113. Zu K, Chau K, Olugbade TO, Pan L, Chow DH, Huang L, Zheng L, Tong W, Li X, Chen Z, He X, Zhang R, Mi J, Li Y, Dai B, Wang J, Xu J, Liu K, Lu J, Qin L (2020) J Mater Sci Technol 63:145
114. Abioye TE, Olugbade TO, Ogedengbe TI (2017) J Emerg Trends Eng Appl Sci 8:225
115. Dang C, Olugbade TO, Fan S, Zhang H, Gao LL, Li J, Lu Y (2018) Vacuum 156:310
116. Abioye TE, Omotehinse IS, Oladele IO, Olugbade TO, Ogedengbe TI (2020) World J Eng 17:87
117. Ogedengbe T, Olugbade TO, Olagunju O (2015) Br J Appl Sci Technol 10:1
118. Sassi W, Boubaker H, Bahar S, Othman M, Ghorbal A, Zrelli R, Hihn JY (2020) J Alloy Compd 828:154437
119. Mohammed T, Olugbade TO, Nwankwo I (2016) J Sci Res Rep 10:1–9
120. Searles JL, Gouma P, Buchheit RG (2001) Metall Mater Trans A 32:2859–2867
121. Engler O, Kuhnke K, Krupp H, Hentschel T (2020) Pract Metallogr 57:545–568
122. Crane CB, Gangloff RP (2015). Corrosion. https://doi.org/10.5006/1766
123. Khullar P, Badilla JV, Kelly RG (2017) Paper presented at the CORROSION 2017, New Orleans, Louisiana, USA
124. Engler O, Hentschel T, Brinkman HJ (2015) IOP Conf Ser Mater Sci Eng 82:012111
125. Sukiman NL, Zhou X, Birbilis N, Hughes A, Mol JMC, Garcia SJ, Zhou X, Thompson GE (2012). IntechOpen. https://doi.org/10.5772/53752
126. Rebecca MB, David J, Allison MA, Leslie GB, Ramgopal T, Jenifer SWL (2019) Int J Fatigue 124:1–9
127. Mofarrehi MM, Javidani XG (2022) J Alloy Compd 781:945–983
128. Pang J, Liu F, Liu J, Tan M, Blackwood D (2016) Corrosion Sci 106:217–228
129. Azarniya A, Hosseini HRM (2015) J Alloys Compd 643:64–73
130. Azarniya A, Hosseini HRM, Jafari M, Bagheri N, Shan D, Zhen L (2012) Aging behavior and microstructure evolution in the processing of aluminum alloys. Microstruct Evol Metal Form, Processes, p 267
131. Omiyale BO, Olugbade TO, Abioye TE, Farayibi PK (2022) Mater Sci Technol 38:391–408
132. Bankong BD, Abioye TE, Olugbade TO, Gbadeyan OO, Zuhailawati H, Ogedengbe TI (2023) Mater Sci Technol 39:129–146
133. Omiyale BO, Ogedengbe II, Olugbade TO, Farayibi PK (2023). 3D Print Addit Manuf. https://doi.org/10.1089/3dp.2022.0253
134. Sassi W, Zrelli R, Hihn JY et al (2020) J Polym Res 27:323
135. Ojo OT, Olugbade TO, Omiyale BO (2021) Anal Techn Szegedinensia 15:8
136. Omiyale BO, Rasheed AA, Akinnusi RO, Olugbade TO (2022) In: Biotechnology—biosensors, biomaterials and tissue engineering—annual volume 2022 [working title]. IntechOpen. https://doi.org/10.5772/intechopen.104465
137. Udensi SC, Ekpe OE, Nnanna LA (2020) Chem Afr 3:303–316
138. Zhang J, Wang W (2020) Chem Afr 3:317–321
139. Zeghaoui S, Hanniche Z, Bouyakoub I et al (2022) Chem Afr 5:673–681